

Supplementary Information

Appearance of the coating specimens before and after the heat treatment in air










| Specimen | LP | MP | HP |
|----------|---|---|---|
| AP → |  |  |  |
| HT400 → |  |  |  |
| HT650 → |  |  |  |

Figure S1. Coating appearance before and after heat treatment. The color of coatings changes due to the oxidation of Ni when the NiP coatings are heat-treated in the presence of oxygen.

The nickel was oxidized in air when heat treated at 400°C. The oxidation level and so-formed oxide layer thickness varied with the treatment temperature and time. Also, the crystallinity behavior of nickel oxide (NiO) changed with temperature and time. The color became sky-blue in a low-phosphorus (HT400-LP) coating, a mixture of sky-blue and greenish yellow in mid-phosphorus (HT400-MP), and greenish yellow in high-phosphorus (HT400-HP) coating specimens when heat-treated at 400°C for 1 hour. Similarly, after 650°C/4 hours heat treatment, the color further turned greenish black in low-phosphorus (HT650-LP) and black in mid- and high-phosphorus (HT650-MP and HT650-HP) coating specimens. Since NiO is an electrochromic material, it is utilized in smart windows and many other applications, such as dye-sensitized solar cells (DSSC). It has been reported that the

stoichiometric NiO color is green, and the non-stoichiometric NiO color is black [1]. The dark color of NiO film is observed due to a $\text{Ni}^{2+}/\text{Ni}^{3+}$ mixed valence state correlated to a Ni_{1-x}O non-stoichiometry created by vacancies or defects [1][2].

Morphology observed from Confocal microscope:

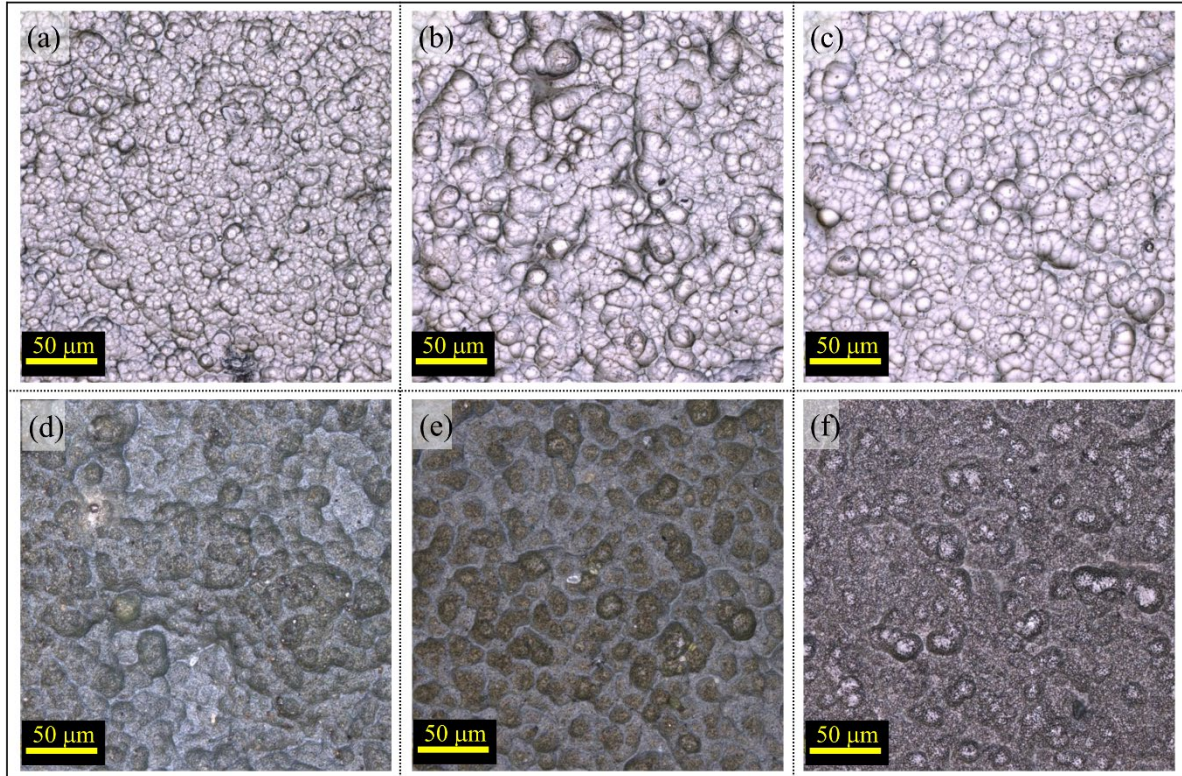


Figure S2. Upper row images are the surface morphology of as-plated Ni-P coatings observed via confocal microscope for (a) AP-LP, (b) AP-MP, and (c) AP-HP specimens. Similarly, the lower row images are the morphologies of 650 °C heat-treated (g) HT650-LP, (h) HT650-MP, and (i) HT650-HP specimens. The scale bar on the images represents 50 μm .

Confirmation of phosphorus segregation in HT650 specimens

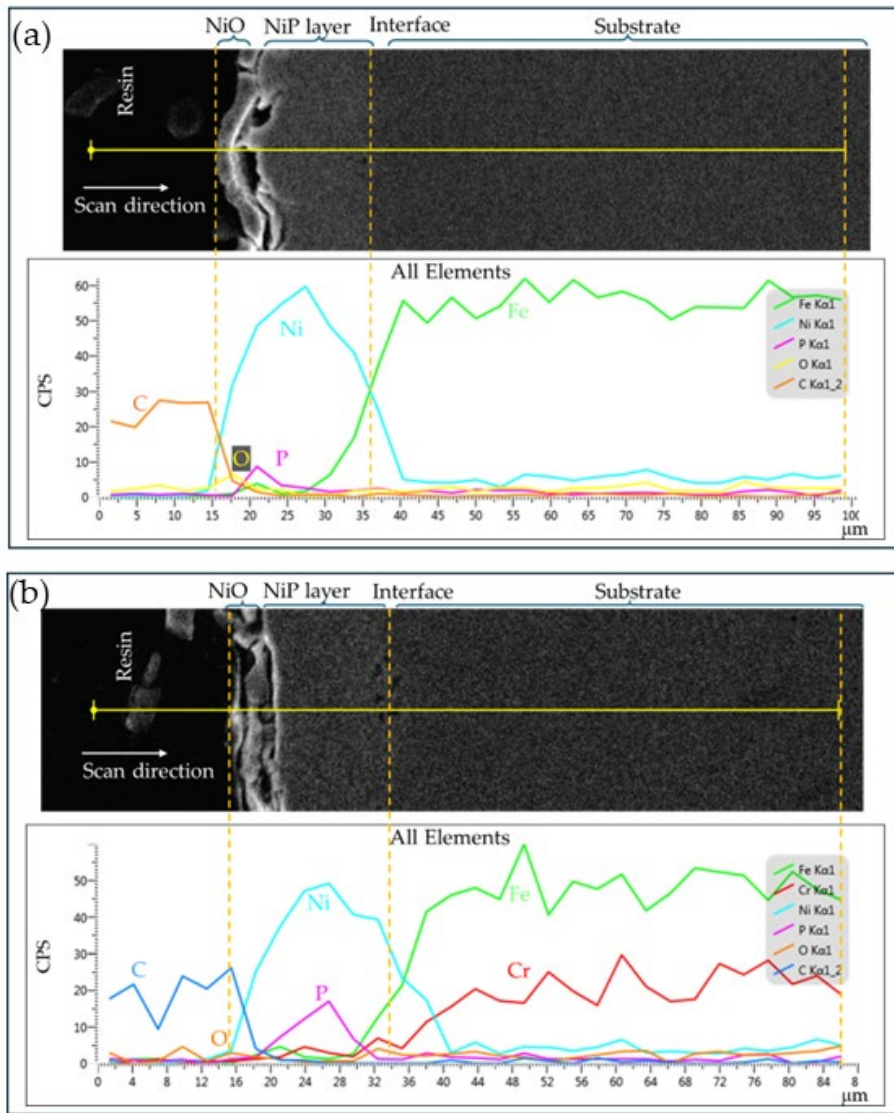


Figure S3. EDS elemental line profile spectra of (a) HT650-LP and (b) HT650-MP specimens. Phosphorus segregation (spiked P spectra) near the top coating surface is observed after the heat treatment at 650°C. Also, Ni and Fe diffusion near the interface region has been noticed in specimens regardless of P-content.

Adhesion test of the coatings

(a) Cross-cut method

The as-plated coating samples and HT400 samples show good adhesion with the ASTM 304SS substrate regardless of phosphorus (P) content. However, HT650 samples show mixed results of adhesion. The results indicate that the Ni oxidation and formation of the nickel oxide layer are affected by the P-content of the Ni-P coatings when heat-treated at 650°C. Notably, the NiO layers created in the HT650 samples with mid- and high-P contents exhibit less adhesion and are brittle, in contrast to the adhesive-type nickel oxide layer seen in the samples with low P content.

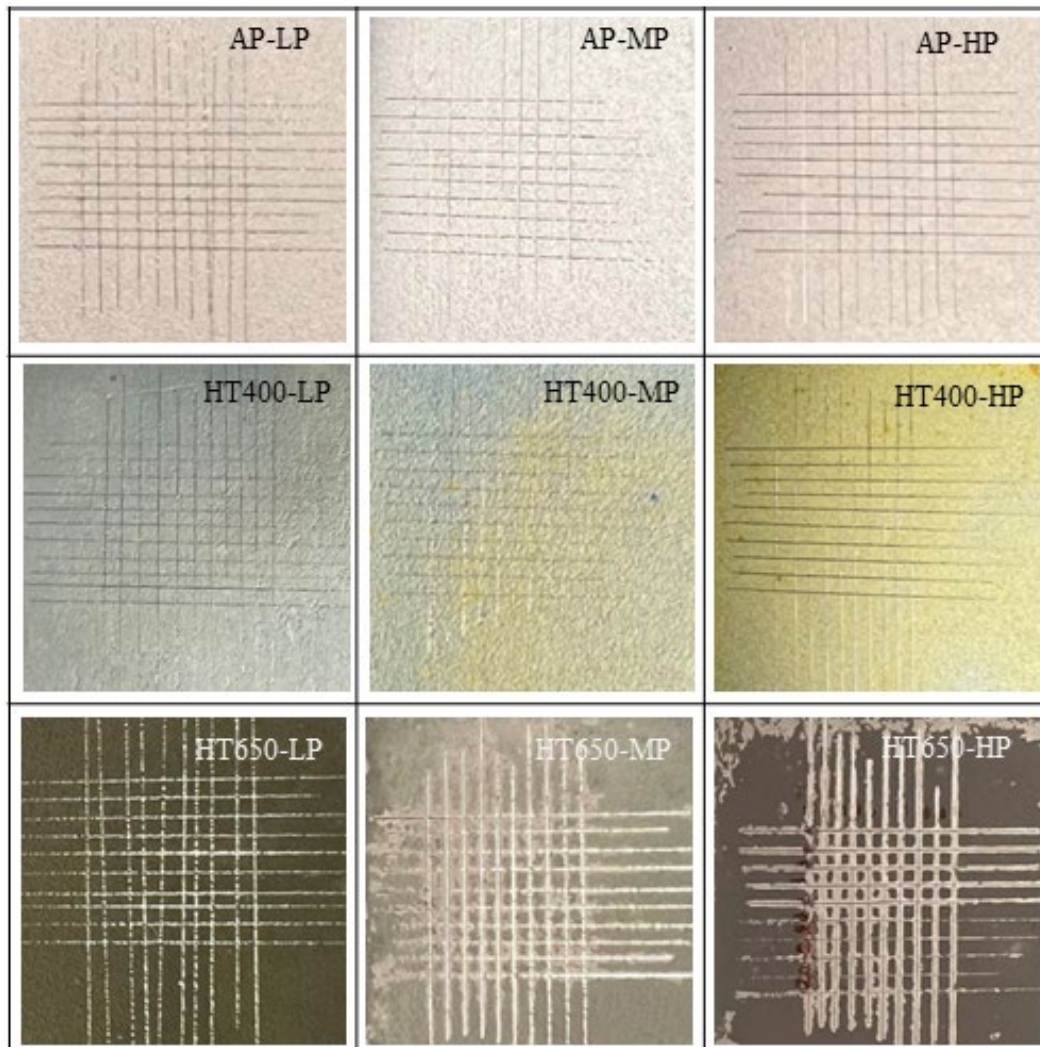


Figure S4. Cross-cut adhesion test of low-, mid-, and high-phosphorus electroless Ni-P coatings in as-plated (AP), heat-treated at 400°C (HT400), and heat-treated at 650°C (HT650) conditions.

(b) Rockwell-indenter scratch test method

The adhesion tests of the coatings were further confirmed by the scratch test using a standard Rockwell diamond indenter (D-275) performed in the progressive load of 1 to 40 N. The scratch test showed similar results as those obtained from the cross-cut method. All the as-plated Ni-P coatings (Figure S5 a-c) demonstrated excellent adhesion with the substrate since there was almost no or very little spallation of coatings seen at the end of the scratch marks where the applied load was maximum (near 40 N). However, debris appeared around the scratch marks on the HT650 specimens due to the spallation of the top NiO layer. It was observed that an increasing quantity of debris was formed in the HT650-MP specimen than in the HT650-LP specimen. The debris quantity was further increased in the HT650-HP specimen indicating the less adhesive nature of the NiO layer. Moreover, there was no evidence of the detachment of the Ni-P layer from the steel substrate as the Fe signals were not observed on the EDS spectra taken at the extreme end of the scratch mark where the applied load was a maximum of 40 N (Figure S6). Therefore, it can be inferred that both as-plated and heat-treated Ni-P layers were excellently adhered to the steel substrate.

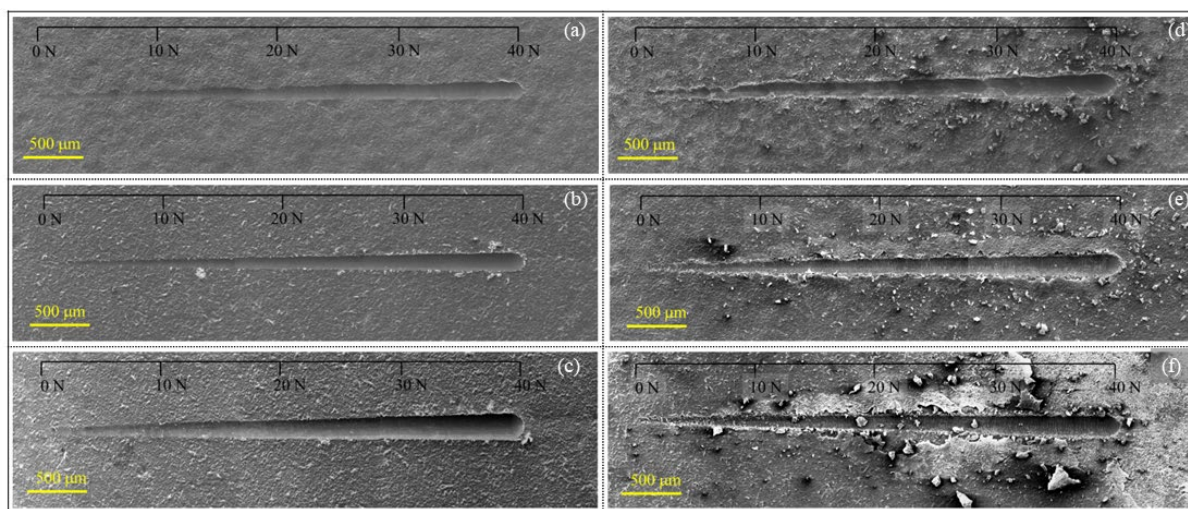


Figure S5. The first column consists of the scratch images of the as-plated coatings (a) AP-LP, (b) AP-MP, and (c) AP-HP. Similarly, the second column consists of the scratch images of the 650 °C heat-treated coatings (d) HT650-LP, (e) HT650-MP, and (f) HT650-HP obtained via SEM after the scratch test using Rockwell (D-275) indenter. A progressive load from 1 to 40 N was applied, and the scratch length was fixed to 4 mm for all the coatings. The scale bar shown in the images represents 500 μm .

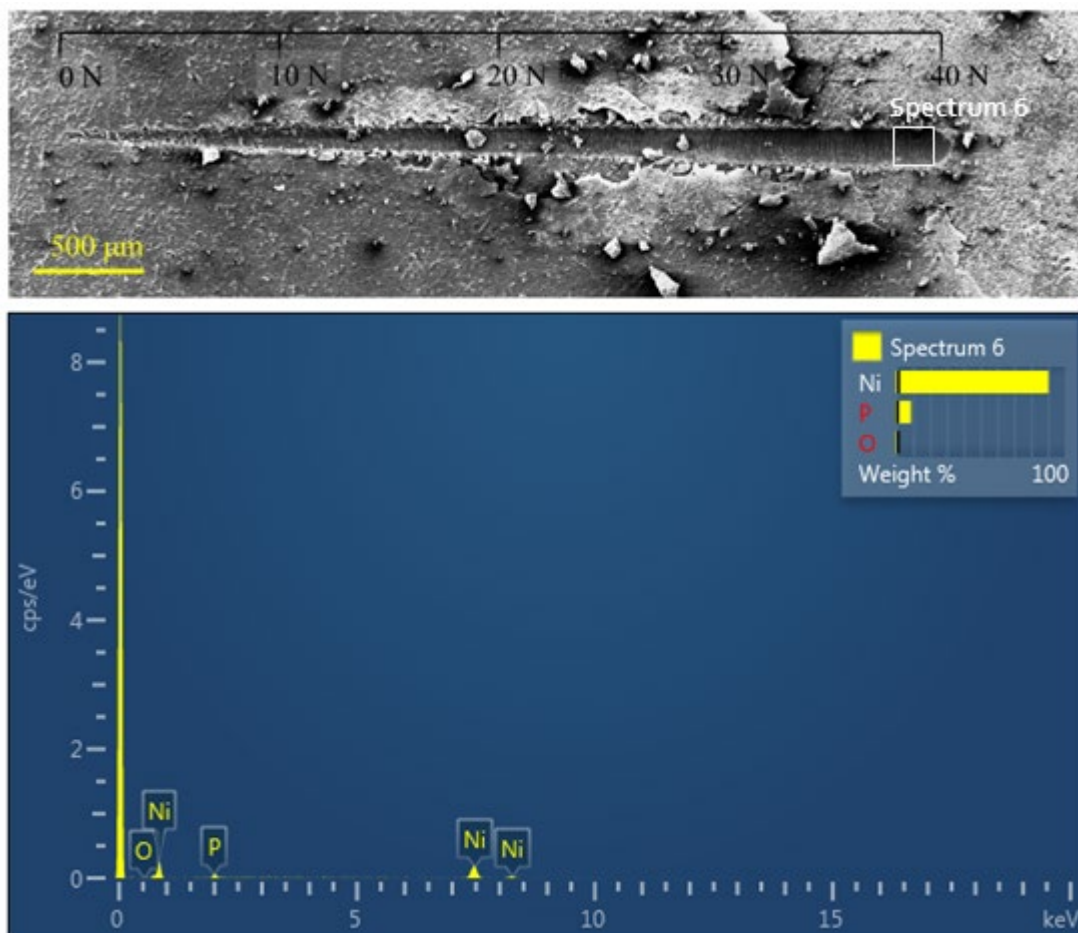


Figure S6. EDS elemental analysis was performed on the extreme end (indicated by a rectangle) of the scratch mark on the HT650-HP specimen where the applied load was maximum. The absence of Fe signals indicates that Ni-P coating was not detached completely from the steel substrate, and the debris around the scratch mark was only from the top (NiO) layer of the coating.

Friction and wear properties of low-, mid-, and high-phosphorus NiP coating heat-treated at 400°C (HT400 specimens):

The figure below shows the COF curves and wear scar images recorded during the sliding wear test of the low-, mid-, and high-phosphorus NiP coatings that are heat-treated at 400°C for 1 hour in an air environment (HT400 specimens). The COF curve of the mid-phosphorus HT400-MP specimen is found to be stable throughout the sliding process. However, fluctuation of COF is seen in the HT400-LP and HT400-HP specimens. Furthermore, a large wear scar appeared in the HT400-LP specimen along with its pair surface as compared to the HT400-MP and HT400-HP specimens. This behavior indicates that the formation of the hard Ni_3P crystallites is predominant in mid- and high-phosphorus NiP coatings. Therefore, excellent wear-resistance properties result after the heat treatment at 400°C.

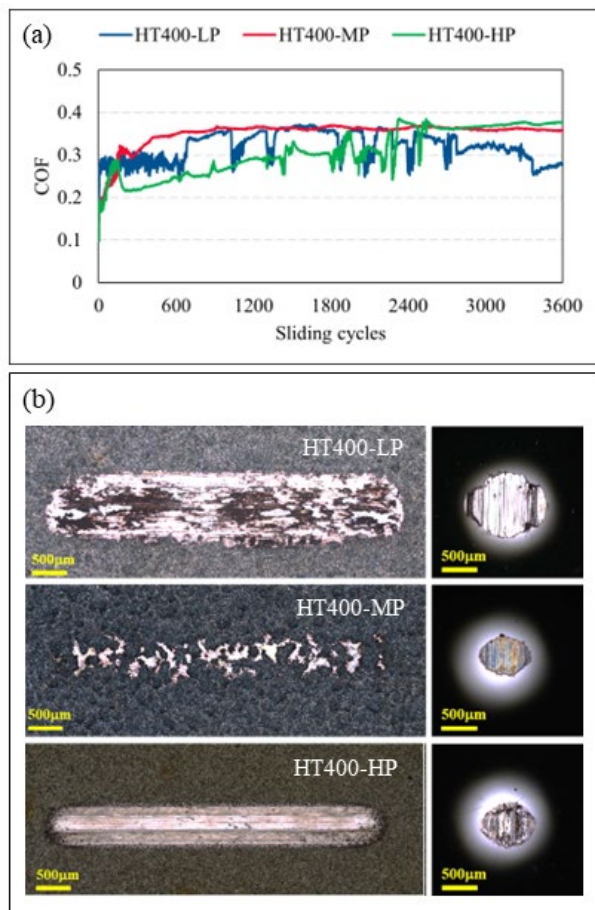


Figure S7. Shows (a) the coefficient of friction curve and (b) confocal microscope images of wear scars observed on the HT400 coating sample and steel ball surfaces after the reciprocating sliding wear test using a 5N load.

Comparison of wear behavior of 304SS substrate and Ni-P coatings:

Figure S8 compares the wear-resistance performance of 304SS substrate and as-plated Ni-P coatings observed at 10 N of applied load. The other conditions of the wear test were the same as those given in the materials and method section of the manuscript. It was found that the Ni-P coatings had enhanced the wear-resistance properties of the 304SS substrate as evidenced by the lower wear volume of the Ni-P coatings. The wear volume of the substrate was 0.135 mm³, whereas it was 0.056 mm³, 0.111 mm³, and 0.128 mm³ in as-plated AP-LP, AP-MP, and AP-HP coating specimens. Low-phosphorus Ni-P coating in its as-plated state (AP-LP) showed promising outcomes of wear resistance properties. However, the mid- and high-phosphorus Ni-P coatings in their as-plated demonstrated a feeble enhancement in wear-resistance behavior compared to the 304SS substrate.

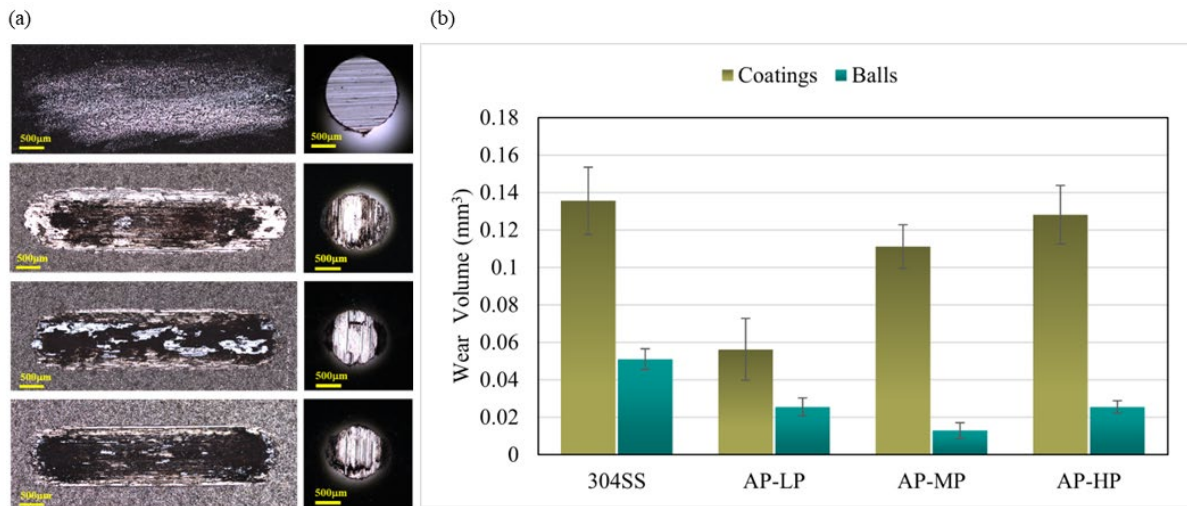


Figure S8. (a) Wear-scar images and (b) wear volume of the 304SS substrate and as-plated coatings obtained when the applied load was 10 N. The wear volume of the 304SS substrate was found to be higher in comparison with the wear volume of the as-plated coatings. Low-phosphorus Ni-P coating in as-plated condition, AP-LP, had shown enhanced wear-resistance properties among the as-plated coatings. The scale bar in the wear images represents 500 μm.

References

1. Mohseni Meybodi, S.; Hosseini, S.A.; Rezaee, M.; Sadrnezhad, S.K.; Mohammadyani, D. Synthesis of Wide Band Gap Nanocrystalline NiO Powder via a Sonochemical Method. *Ultrason Sonochem* **2012**, *19*, 841–845, doi:10.1016/j.ultsonch.2011.11.017.
2. Renaud, A.; Chavillon, B.; Cario, L.; Pleux, L. Le; Szuwarski, N.; Pellegrin, Y.; Blart, E.; Gautron, E.; Odobel, F.; Jobic, S. Origin of the Black Color of NiO Used as Photocathode in P-Type Dye-Sensitized Solar Cells. *Journal of Physical Chemistry C* **2013**, *117*, 22478–22483, doi:10.1021/jp4055457.